APPLIED AND ENVIRONMENTAL MICROBIOLOGY, Apr. 1995, p. 1357–1362 Vol. 61, No. 4
0099-2240/95/$04.00+0

Light Element Analysis of Individual Bacteria by X-Ray Microanalysis

SVEIN NORLAND,* KJELL MAGNE FAGERBAKKE, AND MIKAL HELDAL

Department of Microbiology, University of Bergen, N-5020 Bergen, Norway

Received 21 October 1994/Accepted 26 January 1995

A method based on X-ray microanalysis (XRMA) with the transmission electron microscope for measurement of total amounts of elements in single microbial cells has been developed. All major elements in cells except hydrogen can be measured simultaneously. XRMA provided N/C ratios (means ± standard errors of the mean) for stationary-phase and growing *Escherichia coli* of 0.23 ± 0.01 and 0.30 ± 0.01, respectively, while CHN analysis gave values of 0.276 and 0.307, respectively, for samples from the same cultures. Analyses of free coccoliths from *Emiliana huxleyi* provided weight fractions close to those of $CaCO_3$: 0.35 ± 0.01, 0.15 ± 0.01, and 0.47 ± 0.01 for calcium, carbon, and oxygen, respectively. Calibration is based on monodisperse latex beads and on microdrops of defined compounds. Elements in particles in the size range from 5 fg to 500 pg are measured with a relative precision between 500 and 5,000 ppm, depending on size. As a single-cell method, XRMA avoids the shortcomings of commonly used fractionation techniques associated with bulk methods, which are based on centrifugation or filtration. On the basis of morphology and XRMA, particles may be classified more precisely into groups (e.g., biotic versus abiotic) than is possible by bulk methods. Single-cell elemental analysis may provide insight into topics like nutritional and energetic status, macromolecular composition, and (by multivariate statistics) community structure.

The ecological importance of bacteria in both fresh and marine waters has been recognized during the last 2 decades (1). The change in methods from a general enumeration of bacteria as CFU on solid media (agar plates) to total counts of fluorescent-labelled bacteria in the light microscope increased the bacterial numbers reported by 3 to 4 orders of magnitude (14, 22). This discrepancy between viable counts and total counts of bacteria in water is still an enigma, and some major explanations have been forwarded: a large fraction may be viable but nongrowing or may have reduced capability for colony formation on general solid media, or most of the bacteria seen by total counts are dead cells (32). Most of our knowledge about growth rates and nutritional states of native bacteria originates from size fractionation techniques. Fractionation by filtration or centrifugation is the most commonly used method. Both methods will fractionate particles on the basis of some common property. For filtration, it is size, and for centrifugation, it may be weight or gravitational density. It is common to both techniques that they do not distinguish between biotic and abiotic particles or between living and dead cells. One approach to a further understanding of the physiological status of the unculturable bacterial fraction in water is the use of analytical methods applicable at the single-cell level. Flow cytometry, autoradiography, and X-ray microanalysis (XRMA) may operate on more clearly defined classes of particles, but the information they provide has been more limited or less relevant.

XRMA with the transmission electron microscope (TEM) operated in scanning mode can measure all major elements except for hydrogen in single cells. Several aspects of cellular physiological status can be studied by this technique: (i) cellular C/N/P ratios provide information on environmental nutrient conditions; and (ii) osmotic and energy conversion can be studied by analysis of elements like sodium, potassium, magnesium, chlorine, and calcium, as their internal concentrations and gradients are related to physiological processes in cells. Furthermore, this could allow distinction between living and moribund or dead cells and could even give some measure of activity of living cells.

XRMA was adapted to biological thin sections by Hall's continuum method (19), which yielded relative content (fraction of dry weight) of elements. Heldal et al. (21) extended the method for particles by introducing intensity normalization, which allowed total integrated dry weight and elemental content of single cells to be determined.

Because of the limitations imposed by older beryllium window energy dispersive detectors, elements lighter than sodium were excluded from these analyses. Biologically important elements like carbon, nitrogen, and oxygen can be detected only with newer thin-window or windowless X-ray detectors.

Using a traditional beryllium window, we have previously shown XRMA to be applicable as a single-cell method for elements with atomic numbers as low as that of sodium (21, 29).

In this paper, we report an extension of the method, using a thin-window X-ray detector to include light-element (carbon, nitrogen, and oxygen) analysis of single cells also.

MATERIALS AND METHODS

Latex beads with a nominal diameter of 1.09 μm were obtained from Agar Scientific, Stansted, England. Latex is a polystyrene polymer $[(CH_2)_n]$ with a specific density of 1.05 g/cm^3. Coenzyme A ($Na_3C_{21}H_{36}N_7O_{16}P_3S$, 92% clean; Sigma Chemical Co., St. Louis, Mo.), Ca-β-glycerophosphate ($CaC_3H_6O_2S$), $Mg_2(PO_4)_3 \cdot 3H_2O$ (Fisher Scientific, Pittsburgh, Pa.), KNO_3 (Merck, Darmstadt, Germany), and $K_4[Fe(CN)_6]$ (Merck) were each dissolved in distilled water from a quartz still to a concentration of 100 g/m^3.

Escherichia coli was grown in a low-potassium medium (4.5 mM NaH_2PO_3, 1 mM Na_2HPO_3, 10 mM $NaNO_3$, 1 mM KCl, 10 mM $MgSO_4$). When, after 24 h, the culture had reached stationary phase, samples for XRMA and CHN analysis were taken. The culture was then diluted with 2 parts of 1% nutrient broth (Difco), and new samples were taken after 60 min during the following growth phase.

Free coccoliths from the prymnesiophycean alga *Emiliana huxleyi* were obtained from a mesocosm experiment at the marine biological field station, Espegrend, Norway, during May 1992 (10).

Specimen preparation. Aluminum grids (100 mesh; Agar Scientific) were

* Corresponding author. Mailing address: Department of Microbiology, University of Bergen, Jahnebakken 5, N-5020 Bergen, Norway. Phone: 47 55 21 26 81. Fax: 47 55 32 39 62. Electronic mail address: Svein.Norland@im.uib.no.

supported with a carbon-coated Formvar film and glow discharged (7×10^{-1} torr [ca. 0.9 kPa], 1 min).

Latex beads were suspended in distilled water and added as drops onto grids, giving approximately 20 to 50 beads per grid mesh. Excess water was drained off after 30 to 60 s with filter paper, and the grids were air dried. Calibration compounds were dissolved and sprayed onto grids as microdrops (8). Bacteria and coccolith samples were centrifuged onto grids that were attached to a filter dish by tape sticky on both sides (4). Neither fixatives nor stain was applied prior to XRMA.

CHN analysis. Samples of *E. coli* for CHN analysis were harvested on precombusted GF/F filters, four parallel samples (10 ml), by filtration (10^3 Pa). The filters were dried at 60°C overnight and analyzed for carbon and nitrogen in a CHN analyzer (model 1106; Carlo Erba Strumentazione, Milan, Italy) (21).

TEM X-ray. Electron microscopy and XRMA were done with a JEOL 100CX electron microscope equipped with a scanned-image display and a Tracor Z-Max 30 energy-dispersive spectroscope supported with an Si(Li) crystal detector and a Norvar window for light-element detection. The microscope was operated in scanning transmission mode at a tilt angle of 38°, an accelerating voltage of 80 kV, a beam current of 1.6 nA, a spot size of 6.0 nm, and an accumulation time of 50 s (live time).

All mean ratios $\left(\frac{x}{y}\right)$ given are computed as $\overline{\left(\frac{x}{y}\right)}$ (mean of ratios).

To quantify sources of error, the spectra of eight different film areas adjacent to a bacterium were recorded. In addition, six consecutive analyses of one bacterium and its selected film background were performed.

Physical basis of XRMA. When accelerated electrons interact with matter, high-energy photons (X rays) are emitted (6, 18). Most important in this context are the characteristic X rays which are generated when the incident electrons interact with an electron in one of the electron shells of the specimen atoms. These X rays will have an energy corresponding to differences in energy levels between electron shells of the atoms. As energy differences between electron shells are characteristic for an atom, the energy of its X rays can be used to identify the atom of origin and the intensity of characteristic X rays will convey information on the amount of the element in the specimen.

Incident electrons may also interact with the Coulomb field of the nuclei, producing a continuous distribution of X-ray energies termed white radiation. In spectra, white radiation is seen as a continuous background upon which the characteristic peaks are superimposed.

In the detector, the energies of X-ray photons are converted to voltage pulses with sizes proportional to the levels of the photons' energy, and each pulse is registered as an event in a channel corresponding to its size in a multichannel analyzer, thus producing an X-ray energy spectrum.

Intensity normalization. In scanning transmission mode, the intensity of incident electrons will be inversely proportional to the scanned area, on the assumption of a constant flux of electrons. When thin-film theory applies (33) and the specimen can be confined within the scanned area, the relationship among the main parameters of the analysis is described by the equation

$$m_x = \frac{I_x \cdot A}{C_x \cdot t} \quad (1)$$

where m_x is the mass of element x, I_x is net counts from element x, A is the area scanned (in micrometers), C_x is a calibration constant for element x, and t is the (live) analysis time (in seconds) (21).

In the electron microscope, a gross X-ray spectrum is recorded from an area that tightly circumscribes the specimen. A film spectrum is recorded from a particle-free area in the vicinity of the specimen. The following parameters are measured: the width and length of the scanned area, the width and length of the particle, the angle between the particle's main axis and the tilt axis, and the amplification. All dimensions are measured on the cathode ray tube with a slide gauge. The computational steps are as follows. The two spectra and all measured parameters are stored in a computer, in which the following procedure is performed by a program designed by the authors. (i) The matching spectrum of the supporting film is subtracted from the gross spectrum to produce the net spectrum. (ii) A model white radiation spectrum is adjusted and subtracted from the net spectrum to produce the peak spectrum (modified from reference 21). (iii) The areas (integrated counts) of peaks are estimated. K_α peaks for elements with Z of >8 are processed first, starting with the highest peaks. Peak area is estimated by fitting the central part of the peak (avoiding the tails and possible overlap from neighboring peaks) to a normal distribution. The fit is extrapolated to produce a full normal distribution. This estimated peak is removed from the spectrum by subtraction together with any related peaks (e.g., β peaks, L family peaks, escape peaks, and double peaks). Carbon, nitrogen, and oxygen are resolved last, together, by an iterative simplex routine working on the assumption that their energies and peak widths are known. (iv) Preliminary amounts of elements (in picograms) are calculated from peak areas by equation 1, and mass thickness (in picograms per square micrometer) for elements is estimated. (v) The mass thickness is adjusted for absorption in the specimen by an iterative approximation, based on preliminary mass thickness as a starting point and absorption coefficients for all relevant combinations of emitters and absorbers (18). (vi) The width and length of the particle are adjusted for the distortion caused by the tilt angle. The volume is then estimated on the assumption of a cylindrical shape with a hemisphere at each end (21).

TABLE 1. Fraction of C in latex; amounts of Na, N, O, P, and S relative to C in coenzyme A; and calibration constants determined

Compound	Element	Relative amt (wt/wt)	Calibration constant[a]	
			Value [counts · μm^2/(fg · s)]	% Error
Latex[b]	C	0.86	0.45	1
Coenzyme A[c]	Na	0.27	1.98	9
	N	0.39	0.62	10
	O	1.02	0.78	8
	P	0.37	2.60	6
	S	0.13	2.68	6

[a] C_x in equation 1.
[b] $n = 14$.
[c] $n = 6$.

RESULTS

Calibration was carried out in two steps. First, a calibration constant for carbon was determined from latex beads of known mass. Next, calibration constants for other elements were determined on the basis of their amounts relative to that of carbon in selected compounds. Some calibration constants are shown in Table 1; the calibration constant for carbon was obtained from latex beads, and the calibration constants for nitrogen, oxygen, sulfur, phosphorus, and sodium were obtained from coenzyme A. A peak spectrum for coenzyme A is shown in Fig. 1. Figure 2 shows amounts of nitrogen, oxygen, sulfur, phosphorus, and sodium versus carbon for a series of different-sized microdrops of coenzyme A. By the same procedure, calibration constants for other relevant elements were determined from analyses of microdrops of suitable compounds: that of calcium was determined from Ca-β-glycerophosphate, that of magnesium was determined from $Mg_2(PO_4)_3 \cdot 3H_2O$, that of potassium was determined from KNO_3, and that of iron was determined from $K_4[Fe(CN)_6]$ (data not shown). Calibration constants as a function of the Z values of elements are given in Fig. 3. Calibration constants for elements not included in the calibration procedure were estimated by interpolation of the constants determined for elements with neighboring Z numbers.

Results from XRMA of *E. coli* cells from stationary and growing cultures are summarized as mean values in Table 2. Total dry weight is calculated as the sum of all measurable elements plus a contribution from hydrogen assumed to be 1/6 (wt/wt) that of carbon. *E. coli* cells from growing cultures have a higher cell volume and also a higher relative content of most major elements except carbon than do cells from the stationary phase. Bacteria from the stationary culture have a higher dry-weight-to-volume ratio than cells from the growing culture. Measurable elements not shown constitute less than 5% of the dry weight, with chlorine, sodium, and potassium contributing the most. Magnesium, calcium, and iron each contributed less than 0.5%.

Measurements of *E. coli* from batch culture at the growing and stationary phases by XRMA and CHN methods are as follows (errors given are standard errors of means; $n = 4$; see Table 2 for details regarding growth phase): by XRMA and CHN, respectively, the N/C ratios (wt/wt) were 0.30 ± 0.01 and 0.307 ± 0.001 for cultures at growth phase (25 h) and 0.23 ± 0.01 and 0.276 ± 0.001 for cultures at stationary phase (24 h). The mean carbon mass thickness of eight areas of the film surrounding a bacterium was 65 fg/μm^2, with a standard deviation of 5 fg/μm^2. The film contained 79% carbon and 7%

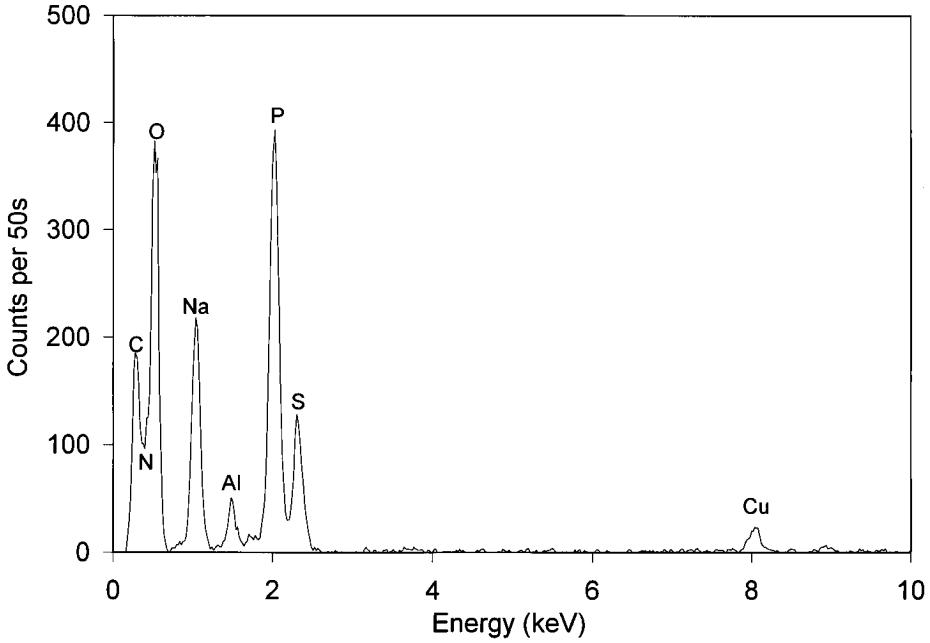

FIG. 1. Net X-ray spectrum of coenzyme A (after subtraction of the film spectrum and the contribution from white radiation).

oxygen, and the sum of other elements measured in the film was less than 1% (assuming that the fraction of hydrogen is 1/6 that of carbon). Repeated analysis of the same bacterium caused no significant change in any of the elements measured. However, the total count of both main and film spectra increased (total film counts increased from 3,000 to 4,400 counts during six repetitions). The contamination is due mainly to deposition of carbon from the microscope.

Mean values (± standard errors of the mean) from the analysis of coccoliths (n = 12) by TEM and XRMA are as follows: length, 3.4 ± 0.2 μm; dry weight, 1,900 ± 300 fg; relative amounts (wt/wt) of C, O, Ca, and other elements, respectively, 0.15 ± 0.01, 0.47 ± 0.01, 0.35 ± 0.01, and 0.030 ± 0.003. The corresponding theoretical values for $CaCO_3$ are 0.12 for C, 0.48 for O, and 0.40 for Ca.

DISCUSSION

On the basis of measurements of latex beads (Table 1), the calibration constant for carbon was determined with a precision better than 1%. The calibration constants for other elements determined from microdrops of acetyl-coenzyme A

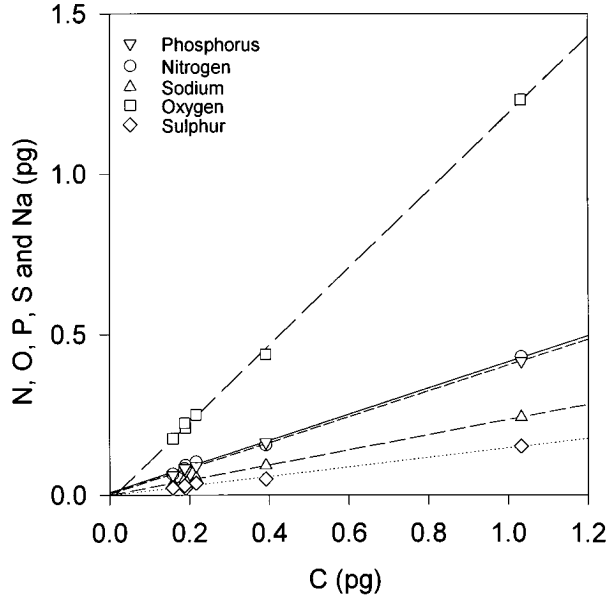

FIG. 2. Amounts of N, O, P, S, and Na versus the amount of C in a series (n = 6) of coenzyme A droplets of different sizes.

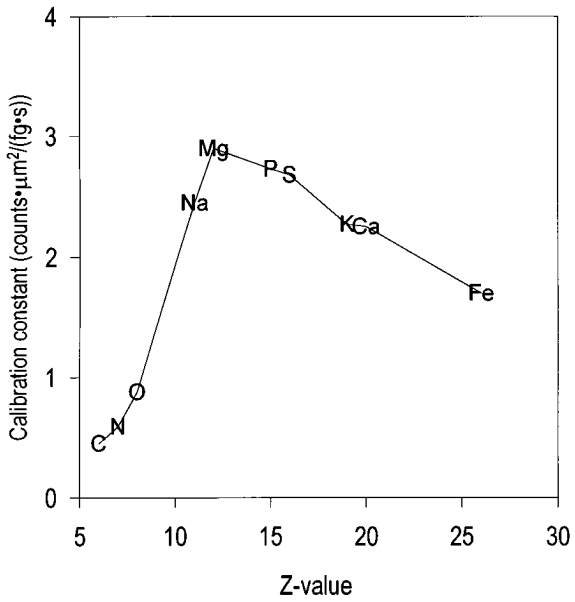

FIG. 3. Calibration constants as a function of Z value for elements included in the calibration procedure.

TABLE 2. Summary of data obtained by X-ray analysis of single cells from an *E. coli* culture in growing and stationary phases[a]

Phase	Vol (μm^3)	Dry wt/vol ($fg/\mu m^3$)	Indicated elemental content as fraction of total (wt/wt)				
			C	N	O	P	S
Growth[b]	4.2 ± 0.4	180 ± 10	0.48 ± 0.01	0.143 ± 0.004	0.176 ± 0.006	0.046 ± 0.001	0.014 ± 0.001
Stationary[c]	0.9 ± 0.2	280 ± 30	0.59 ± 0.01	0.136 ± 0.006	0.131 ± 0.003	0.037 ± 0.001	0.010 ± 0.001

[a] All values are means ± standard errors of the mean.
[b] $n = 25$; 25 h.
[c] $n = 20$; 24 h.

were all determined with a precision better than 10% (Table 1). The loss of precision in the second calibration step is in part explained by the uncertainty with which carbon is determined in these samples. The net carbon peak is most influenced by errors introduced by subtraction of the contribution from the supporting film, as the film spectrum has a pronounced carbon peak. It is not possible to distinguish a separate nitrogen peak in Fig. 1. However, as the energy and width of the nitrogen peak are precisely known, its area can be determined with satisfactory precision by deconvolution.

Other calibration compounds, e.g., Ca-β-glycerophosphate, give similar values for calibration constants for phosphorus and oxygen. Still, statistically significant compound-to-compound variation between calibration constants occurs. This could be due either to impurities of the compounds or to variable mass loss during analysis (2).

From Table 2, carbon-to-volume values of 90 and 170 $fg/\mu m^3$ for *E. coli* growth phase and stationary phase, respectively, may be computed. These are in accordance with values from Watson et al. (37), Luria (27), and Bakken and Olsen (3) but lower than the conversion factor between volume and carbon frequently used in ecological studies (25). It should be noted that the method presented in this study will give values for amount of carbon (or any other element) per cell directly and not via volume estimates, which are inaccurate and dependent upon the method of measurement (20). Furthermore, it is recognized that the carbon-to-volume ratio varies with size as well as temporally and geographically (24).

The measured fractions of carbon and nitrogen (see above) are close to those reported by Luria (27) and Ingraham et al. (23). The data above show that XRMA yields precise (3 to 4% error) mean N/C ratios for *E. coli*, implying that a small number of analyses may be sufficient to detect significant differences between samples. XRMA and CHN give significantly different results for cells from the stationary culture. The higher N/C ratio obtained by CHN in stationary phase may be due to presence of extracellular, nitrogen-rich material retained by the filter. However, too much interpretation should not be put into this difference, as the value from XRMA carries a 10% error from the calibration constant of nitrogen. The N/C ratios are in the range reported previously for bacteria: 0.26 for freshwater bacteria (13) and 0.27 for marine bacteria (26).

The fractions of oxygen (0.176 and 0.131) are lower than those given by Luria (27), who reported a value of 0.2 estimated by difference. To our knowledge, the values given in this study are the first direct estimates of the oxygen fraction in microorganisms.

The cellular fraction of phosphorus was high, a finding which is reasonable as this element is in excess in the growth medium. Still, it was within the wide range of values reported for bacteria (5, 9, 17, 34, 36).

Sulfur fractions for *E. coli* were reported by Luria (27) to be 1.1% and by Dyson (9) and Ingraham et al. (23) to be 1%. All of these values for sulfur fractions in the bacteria are high, considering that Cuhel et al. (7) found the sulfur content in bacterial protein to be 1.1%. The nonprotein sulfur fraction in marine bacteria has been estimated to be 20% (7), while significantly higher fractions have been reported for some algae (28).

The analyses of *E. coli* showed significant differences between stationary-phase and growth phase cells for all parameters except nitrogen (Table 2). As would be expected, growing cells are larger and have a relatively higher content of elements (phosphorus and sulfur) found in growth-related macromolecules like proteins and nucleic acids. Conversely, stationary-phase cells have a higher carbon fraction and a lower oxygen fraction, suggesting a macromolecular composition richer in fats.

The molecular composition of the cell is dominated by a few types of macromolecules with known elemental compositions (Table 3). An approximate inventory of the macromolecular composition of these cells can be made from the matrices of Tables 2 and 3 plus a few assumptions (16): (i) in this context, macromolecules also include low-molecular-weight precursors; (ii) only a fraction (here assumed to be 50%) of sulfur in the cells is associated with protein; and (iii) the cell does not include compounds like calcite, silica, or metallo-oxides.

The estimated mass fractions of macromolecules are given in Table 4. The negative fractions for carbohydrates suggest that there is a deficit of oxygen in our analysis, probably caused by mass loss under the electron beam (2). The oxygen fractions must be adjusted to 0.26 and 0.24 for growing and stationary cells, respectively, to give zero carbohydrate content. This would also reduce the fractions of fat to 0.05 and 0.23, respectively. Escaping oxygen may be accompanied by other elements like carbon (e.g., as CO_2). If this is the case, the carbon fraction will also have to be adjusted although to a lesser degree. As protein is the only sulfur-containing macromolecule (Table 3), the uncertainty of the sulfur fraction (both the fraction actually associated with protein and that associated with the calibration constant of sulfur) will contribute to the uncertainty of the protein fraction and also to that of the fraction of nucleic acids,

TABLE 3. Approximate relative elemental composition of macromolecules

Element	Approximate relative elemental composition (wt/wt) of macromolecules of[a]:				
	Proteins	Carbohydrates	Fats	Nucleic acids	Polyphosphates
C	0.52	0.40	0.80	0.38	0.00
N	0.16	0.00	0.00	0.17	0.00
O	0.22	0.53	0.08	0.31	0.61
P	0.00	0.00	0.00	0.10	0.39
S	0.01	0.00	0.00	0.00	0.00

[a] See reference 16.

TABLE 4. Estimated relative macromolecular composition of *E. coli* computed from values in Tables 2 and 3

Phase	Relative macromolecular composition (wt/wt) of organism				
	Proteins	Carbohydrates	Fats	Nucleic acids	Polyphosphates
Growth	0.71	−0.17	0.15	0.17	0.08
Stationary	0.49	−0.22	0.37	0.34	0.01

with which protein shares the available nitrogen. The estimated sum of protein and nucleic acid quantities will hence be more reliable than a determination made from the quantities of each of the two components taken separately.

The data from the analyses of coccoliths (above) yielded results that are close to those for $CaCO_3$ but still significantly different. Contrary to the *E. coli* results, there is no deficit of oxygen; rather, there might be a small excess of carbon and oxygen relative to calcium, suggesting the presence of a carbohydrate envelope or matrix (12).

Preparation of cells. The purpose of the preparation technique is to bring the organism from its environment onto the grid surface with a minimum of perturbation. Harvesting of samples directly onto grids by centrifugation has been shown to be a gentle and quantitative method (4). Furthermore, use of fixatives and stains should be avoided. Fixatives will make membranes permeable and thus destroy any concentration gradients over the cell membrane (unpublished results). This may cause a significant reduction of the cell volume (15, 35). Washing with low-molarity solutions should be avoided, especially for cells harvested from marine environments. Once cells are air dried on a grid surface they may be kept unchanged for several months (unpublished observation).

Staining will interfere with the analysis of elements and introduce uncontrollable artifacts into the analysis.

Limitations and errors. The method relies on a rigorous control of the flux of accelerated electrons through the scanned area. A certain relative deviation in the flux will effect all absolute measures proportionally. With the equipment used, we found that this control was best achieved with monodisperse latex beads as an internal standard, and we adjusted all elements proportionally to the deviation observed for carbon in latex. Absorption of X rays within the specimen will set the upper size limit for analysis. At a dry weight of 500 pg (organism diameter, ca. 20 μm), the fraction of the K_α nitrogen photons that escape the specimen becomes so small that the absorption correction becomes imprecise.

The lower mass limit (approximately 5 fg [total dry weight]) is determined by the radiation damage caused by the high doses applied to small cells but also by scarcity of counts and by variability of the thickness of the supporting film.

On the assumption of proportionality between mass and volume, mass thickness (mass per unit area) will be proportional to linear size (equation 1). The standard deviation of carbon mass thickness (SD_{CF}), 5 fg of C per μm^2, is too large to be explained by counting statistics alone; to some extent this may also be true of oxygen. The main part of the variation is due to uneven film thickness, implying that a longer accumulation time will not improve the precision of the measurement of carbon. The relative error introduced into the carbon measurement of the specimen is the ratio between SD_{CF} and the mass thickness of the specimen. The relative error introduced into the specimen carbon estimates by SD_{CF} will be inversely proportional to the carbon mass thickness of the specimen. With the detection limit of carbon defined as a relative error equal to 0.5, the smallest detectable specimen mass thickness of carbon is 10 fg/μm^2. On the basis of a carbon-to-volume ratio of 100 fg/μm^3 for the specimen, the lowest detectable amount of carbon is estimated to be ca. 1 fg. However, this estimate is sensitive to both film thickness and the carbon-to-volume ratio of the specimen.

Because of low counts from both the specimen and the film background, the error in the determination of other elements is dominated by counting statistics. The standard deviation of the counts in the peak may be estimated as $SD_E = \sqrt{[P + 2 \cdot (W + F)]}$, where P, W, and F are the counts in the peak, in white radiation, and in film, respectively. With the procedure described, the number of film counts, F, under a peak is typically between 20 and 50 depending on film thickness. The counts from white radiation, W, will depend on specimen size, but for bacteria the number will be in the range 5 to 60. Both W and F will depend on the X-ray energy (element). If, as an example, $W + F$ is set to 50 and the detection limit is defined as a relative error equal to 0.5, the smallest detectable peak will have 20 counts. The lowest mass thickness detectable for an element may be estimated at 0.1 fg/μm^2 [where $C_x = 2$ counts $\cdot$ μm^2/(fg $\cdot$ s) in equation 1]. Because C_x and $W + F$ have similar levels of dependence on X-ray energy, the estimated value will be less dependent on energy. For a bacterial cell of the size of *E. coli*, this corresponds to a relative detection limit of approximately 1,000 ppm (wt/wt). For a small specimen ($W \ll F$), the relative detection limit will be inversely proportional to mass thickness, while that for $W \gg F$ will be inversely proportional to the square root of the mass thickness. Small bacteria (5 fg [dry weight]) will have a detection limit of approximately 5,000 ppm, while larger specimens (500 pg) will have a detection limit of 500 ppm. Thinner supporting film and, to a lesser extent, longer accumulation times will improve this detection limit. Carbon will deposit on the analyzed area during prolonged analysis, but it does so to the same extent for the specimen and the film. Mass loss has been observed for collodion film and possibly also for chlorine in some samples.

Low-temperature analysis with a cryogenic stage may reduce the dose-dependent loss of specimen mass observed in some of our analyses.

Biometrics. Under the electron microscope, the morphometric characteristics of particles form the basis for separation of individuals into groups like bacteria, flagellates, protozoans, and abiotic particles (shells, etc.) (31). Since no staining is applied, the quality of the morphometric information is suboptimal and it is not easy to class some morphometric types; e.g., a 1-μm coccal, unflagellated organism could be a bacterium, a cyanobacterium, or a small eukaryote. Moreover, no morphometric characters allow one to distinguish a flagellated autotroph from a flagellated heterotroph.

XRMA with size measurement in TEM is a single-cell technique that relates all primary data, morphometric characters as well as elemental contents (as many as 15 different parameters), to individual particles or organisms. This allows studies of the interdependence of pairs of variables (correlation) for populations, e.g., the dependence of dry weight or carbon on volume (30), as well as more complex multivariate dependencies (11).

As the cell volume is calculated, the concentration of ions like Na^+, K^+, Mg^{2+}, and Cl^- in cells can also be estimated, allowing osmotic and energetic properties of individual cells and populations to be studied.

ACKNOWLEDGMENTS

This study was supported by the Norwegian Research Council, contracts 104330/720 (K.M.F. and M.H.) and MAS2-CT92-0031 (through Frede Thingstad, to M.H.).

The electron microscopy work was done at the Laboratory for Electron Microscopy, University of Bergen.

REFERENCES

1. **Azam, F., T. Fenchel, J. S. Gray, L. A. Meyer-Reill, and F. Thingstad.** 1983. The ecological role of water-column microbes in the sea. Mar. Ecol. Prog. Ser. **10:**257–263.
2. **Bahr, G. F., F. B. Johnson, and E. Zeitler.** 1965. The elementary composition of organic objects after electron irradiation. Lab. Invest. **14:**1115.
3. **Bakken, L. R., and R. A. Olsen.** 1983. Buoyant densities and dry-matter contents of microorganisms: conversion of a measured biovolume into biomass. Appl. Environ. Microbiol. **45:**1188–1195.
4. **Børsheim, K. Y., G. Bratbak, and M. Heldal.** 1990. Enumeration and biomass estimation of planktonic bacteria and viruses by transmission electron microscopy. Appl. Environ. Microbiol. **56:**352–356.
5. **Bratbak, G.** 1985. Bacterial biovolume and biomass estimations. Appl. Environ. Microbiol. **49:**1488–1493.
6. **Chandler, J. A.** 1976. X-ray microanalysis in the electron microscope, p. 338–339. *In* A. M. Glauert (ed.), Practical methods in electron microscopy. North-Holland Publishing Co., Amsterdam.
7. **Cuhel, R. L., C. D. Taylor, and H. W. Jannasch.** 1982. Assimilatory sulfur metabolism in marine microorganisms: considerations for the application of sulfate incorporation into protein as a measurement of natural population protein synthesis. Appl. Environ. Microbiol. **43:**160–168.
8. **Davis, T. W., and A. J. Morgan.** 1976. The application of X-ray analysis in the electron analytical microscope (T.E.A.M.) to the quantitative bulk analysis of biological microsamples. J. Microsc. **107:**47–54.
9. **Dyson, R. D.** 1974. Cell biology: a molecular approach. Allyn and Bacon, Inc., Boston.
10. **Egge, J. K., and D. L. Aksnes.** 1992. Silicate as regulating nutrient in phytoplankton competition. Mar. Ecol. Prog. Ser. **83:**281–289.
11. **Fagerbakke, K. M., M. Heldal, and S. Norland.** 1991. Variation in elemental content among and within trichomes in *Nostoc calcicola* 79WA01 measured by x-ray microanalysis. FEMS Microbiol. Lett. **81:**227–232.
12. **Fagerbakke, K. M., M. Heldal, S. Norland, B. R. Heimdal, and H. Båtvik.** Chemical composition and size of coccoliths from enclosure experiments and a Norwegian fjord. Sarsia, in press.
13. **Finlay, B. J., and G. Uhlig.** 1981. Calorific and carbon values of marine and freshwater Protozoa. Helgol. Meeresunters. **34:**401–412.
14. **Fry, J. C., and T. Zia.** 1982. Viability of heterotrophic bacteria in freshwater. J. Gen. Microbiol. **128:**2841–2850.
15. **Fuhrman, J. A.** 1981. Influence of method on the apparent size distribution of bacterioplankton cells: epifluorescence microscopy compared to scanning electron microscopy. Mar. Ecol. Prog. Ser. **5:**103–106.
16. **Gnaiger, E., and G. Bitterlich.** 1984. Proximate biochemical composition and caloric content calculated from elemental CHN analysis: a stoichiometric concept. Oecologia (Berlin) **62:**289–298.
17. **Goldman, J. C., D. A. Caron, and M. R. Dennett.** 1987. Regulation of gross growth efficiency and ammonium regeneration in bacteria by substrate C:N ratio. Limnol. Oceanogr. **32:**1239–1252.
18. **Goldstein, J. I., D. E. Newbury, P. Echlin, D. C. Joy, C. Fiori, and E. Lifskin.** 1981. Scanning electron microscopy and X-ray microanalysis, p. 348. Plenum Publishing Corp., New York.
19. **Hall, T. A.** 1971. The microprobe assay of chemical elements, p. 157–175. *In* G. Oster (ed.), Physical techniques in biomedical research, vol. 1A, 2nd ed. Academic Press, Inc., New York.
20. **Heldal, M., S. Norland, G. Bratbak, and B. Riemann.** 1994. Determination of bacterial cell number and cell volume by means of flow cytometer, transmission electron microscopy, and epifluorescence microscopy. J. Microbiol. Methods **20:**255–263.
21. **Heldal, M., S. Norland, and O. Tumyr.** 1985. X-ray microanalytic method for measurement of dry matter and elemental content of individual bacteria. Appl. Environ. Microbiol. **50:**1251–1257.
22. **Hobbie, J. E., R. J. Daley, and S. Jasper.** 1977. Use of Nuclepore filters for counting bacteria by fluorescence microscopy. Appl. Environ. Microbiol. **33:**1225–1228.
23. **Ingraham, J. L., O. Maaloe, and F. C. Neidhardt.** 1983. Growth of the bacterial cell. Sinauer Associates, Inc., Sunderland, Mass.
24. **Kroer, N.** 1994. Relationship between biovolume and carbon and nitrogen content of bacterioplankton. FEMS Microbiol. Ecol. **13:**217–224.
25. **Lee, S.** 1993. Measurement of carbon and nitrogen biomass from naturally derived marine bacterioplankton, p. 319–325. *In* P. F. Kemp, B. F. Sherr, E. B. Sherr, and J. J. Cole (ed.), Handbook of methods in aquatic microbial ecology. Lewis Publishers, London.
26. **Lee, S., and J. A. Fuhrman.** 1987. Relationships between biovolume and biomass of naturally derived marine bacterioplankton. Appl. Environ. Microbiol. **53:**1298–1303.
27. **Luria, S. E.** 1960. The bacterial protoplasm: composition and organization, p. 1–34. *In* I. C. Gunsales and R. Y. Stainier (ed.), The bacteria, vol. 1. Academic Press, Inc., New York.
28. **Matrai, P. A., and M. D. Keller.** 1994. Total organic sulfur and dimethylsulfoniopropionate in marine phytoplankton: intracellular variations. Mar. Biol. (Berlin) **119:**61–68.
29. **Nissen, H., M. Heldal, and S. Norland.** 1987. Growth, elemental composition, and formation of polyphosphate bodies in Vibrio natriegens cultures shifted from phosphate-limited to phosphate-pulsed media. Can. J. Microbiol. **33:**583–588.
30. **Norland, S., M. Heldal, and O. Tumyr.** 1987. On the relation between dry matter and volume of bacteria. Microb. Ecol. **13:**95–101.
31. **Olsen, Y., A. Jensen, H. Reinertsen, K. Y. Børsheim, M. Heldal, and A. Langeland.** 1986. Dependence of the rate of release of phosphorus by zooplankton on the P:C ratio in the food supply, as calculated by a recycling model. Limnol. Oceanogr. **31:**34–44.
32. **Rehnstam, A.-S., S. Bäckman, D. C. Smith, F. Azam, and Å. Hagstrøm.** 1993. Blooms of sequence-specific culturable bacteria in the sea. FEMS Microbiol. Ecol. **102:**161–166.
33. **Roomans, G. M.** 1980. Quantitative X-ray microanalysis of thin sections, p. 401–453. *In* M. H. Hyatt (ed.), X-ray microanalysis in biology. University Park Press, Baltimore.
34. **Tezuka, Y.** 1990. Bacterial regeneration of ammonium and phosphate as affected by carbon:nitrogen ratio of organic substrates. Microb. Ecol. **19:** 227–238.
35. **Trueba, F. J., and C. L. Woldringh.** 1980. Changes in cell diameter during division cycle of *Escherichia coli*. J. Bacteriol. **142:**869–878.
36. **Vadstein, O., A. Jensen, Y. Olsen, and H. Reinertsen.** 1988. Growth and phosphorus status of limnetic phytoplankton and bacteria. Limnol. Oceanogr. **33:**489–503.
37. **Watson, S. W., T. J. Novitsky, H. L. Quinby, and F. W. Valois.** 1977. Determination of bacterial number and biomass in the marine environment. Appl. Environ. Microbiol. **33:**940–946.